

Supplementary material to:
Improvements of organic aerosol representations and their
effects in large-scale atmospheric models

H. Tost and K. J. Pringle

April 11, 2012

1 OC burdens

1.1 Column burdens

The total hydrophilic OC column burdens (in mg/m²) are almost similar in all 5 simulations and are presented below.

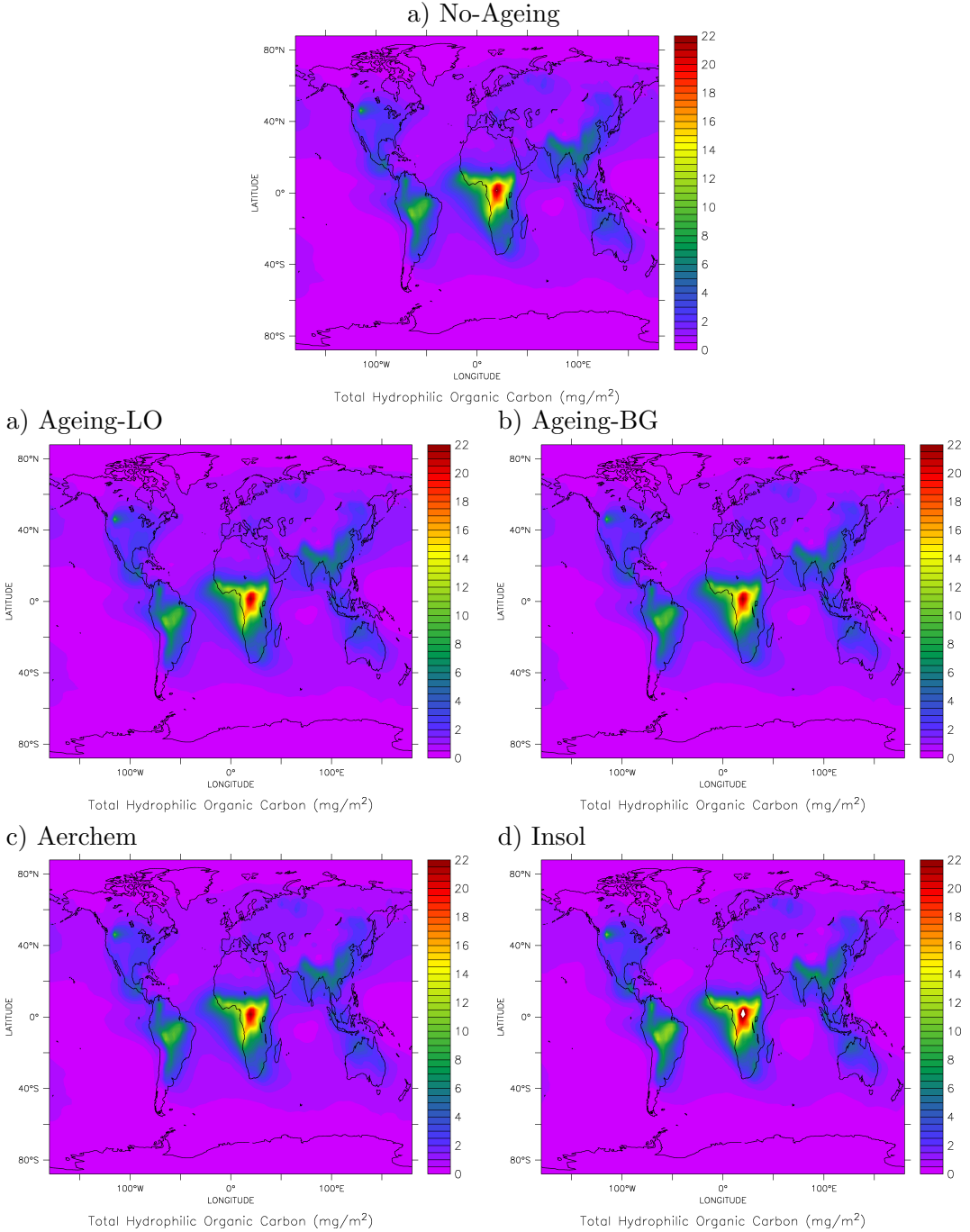


Figure 1: Total OC column burdens in mg/m² for the five simulations. For all except the *No-ageing* simulation the contributions from all OC tracers are added. For the *Aerchem* simulation contributions of dissolved compounds are not taken into account here.

1.2 Surface mixing ratios

This graph displays the surface mixing ratios of the total hydrophilic OC (in nmol/mol), again showing only small differences between the simulations within the typical range of uncertainty in comparison with observations as shown in Pringle et al. (2010).

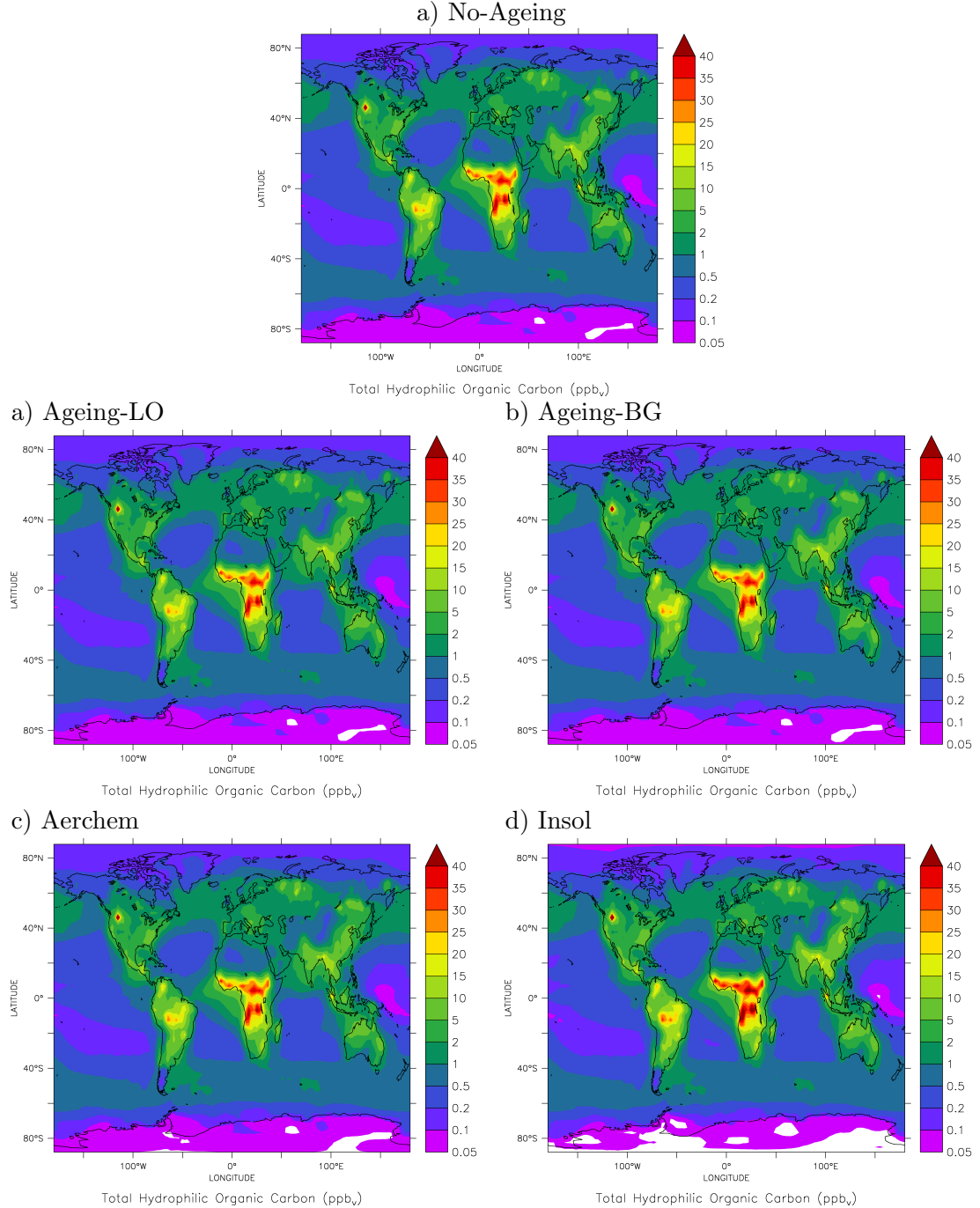


Figure 2: Annual average of the total hydrophilic OC surface mixing ratios in nmol/mol for the five simulations. For all except the *No-ageing* simulation the contributions from all OC tracers are added. For the *Aerchem* simulation contributions of dissolved compounds are not taken into account here.

2 OH concentrations

The concentrations of the main oxidant OH are shown for the *Ageing-BG* simulation. Since the OH is not consumed in the organic aerosol ageing process, the concentrations are similar in all simulations, and only small differences occur due to indirect feedbacks of the aerosol size distribution and interactions with other compounds, e.g. HNO_3 and NO_3^- . The OH concentrations indicate regions in which quick ageing occurs, and the speed of

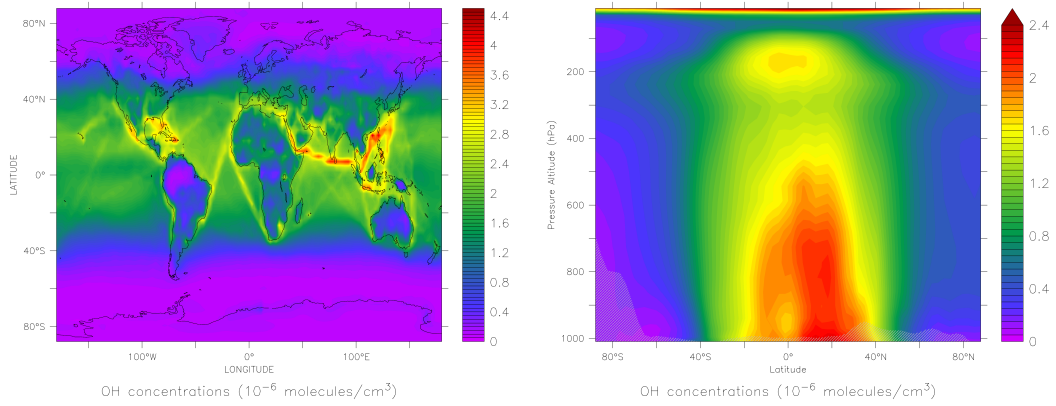


Figure 3: Annual average of the surface and zonal average OH mixing ratios.

the ageing due to the OH exposure time.

3 Fractionation of OC compounds at the surface

This section shows the relative contribution of each of the OC compounds to the total OC.

3.1 Ageing-*LO* simulation

3.1.1 Hydrophilic Aitken mode

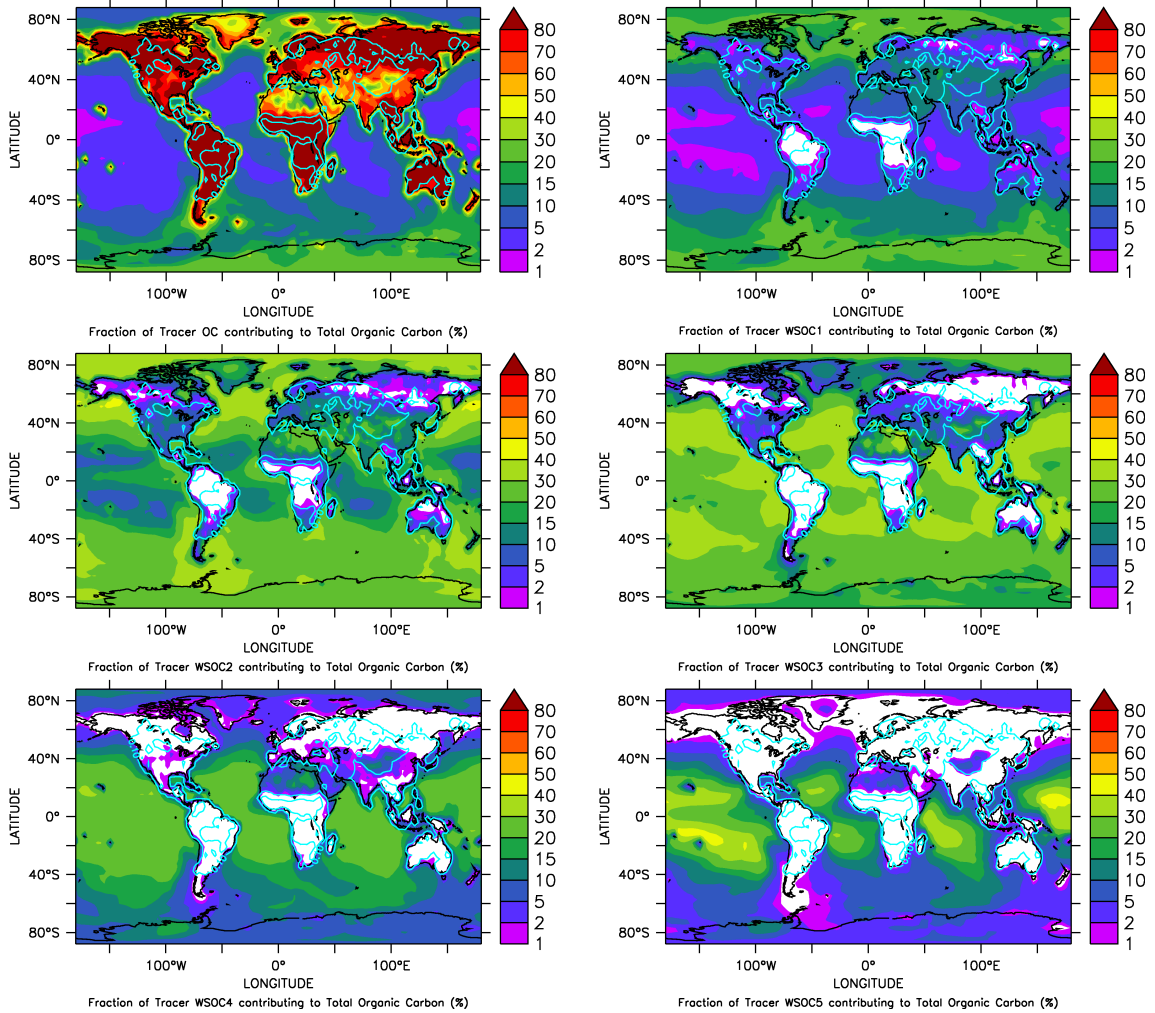


Figure 4: Annual average of the relative contribution of the different organic aerosol compounds to the total organic carbon in the surface layer. The turquoise colored line represents the total organic carbon in the layer.

3.1.2 Hydrophilic Accumulation mode

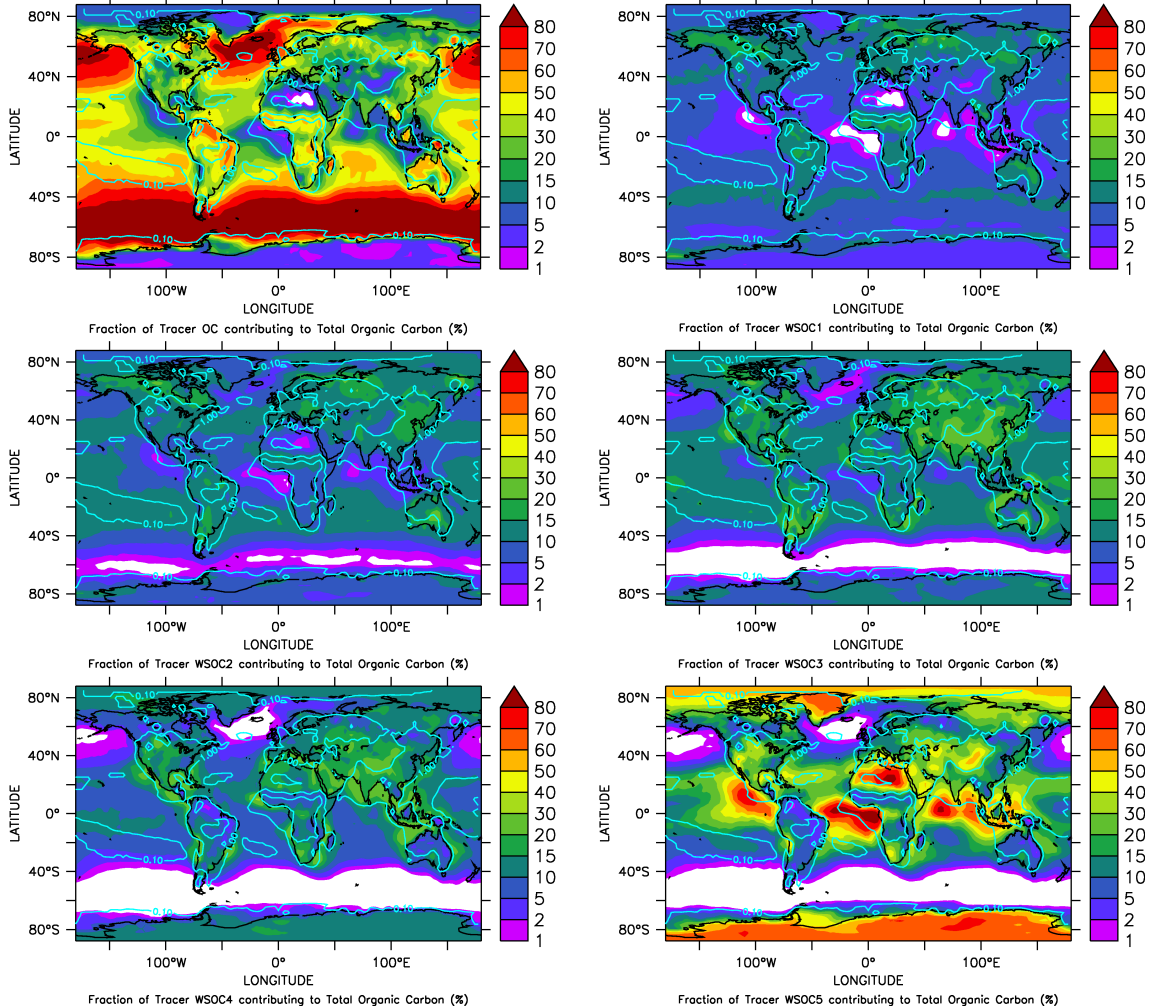


Figure 5: Annual average of the relative contribution of the different organic aerosol compounds to the total organic carbon in the surface layer. The turquoise colored line represents the total organic carbon in the layer.

3.1.3 Hydrophilic Coarse mode

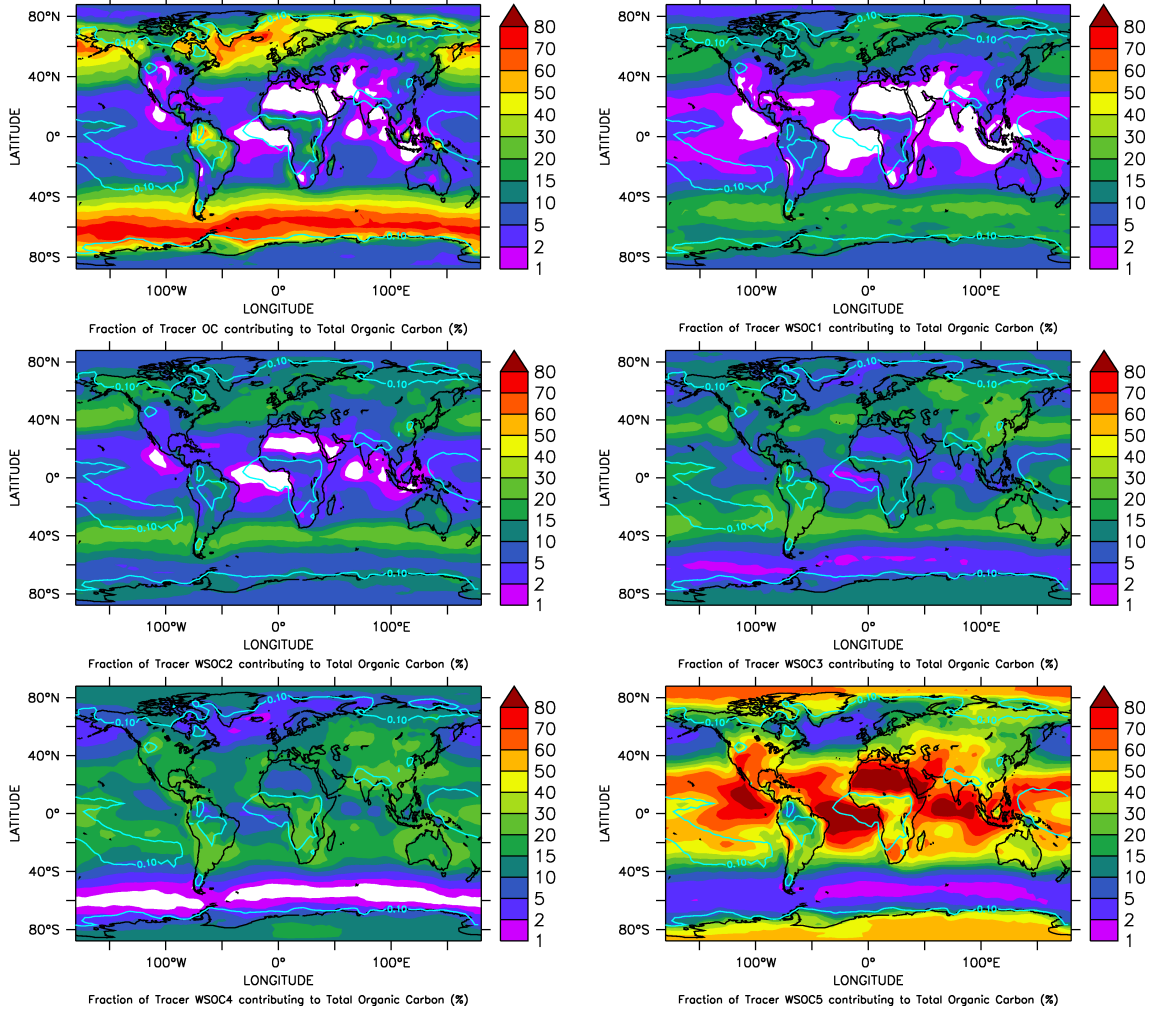


Figure 6: Annual average of the relative contribution of the different organic aerosol compounds to the total organic carbon in the surface layer. The turquoise colored line represents the total organic carbon in the layer.

3.2 Ageing-BG simulation

3.2.1 Hydrophilic Aitken mode

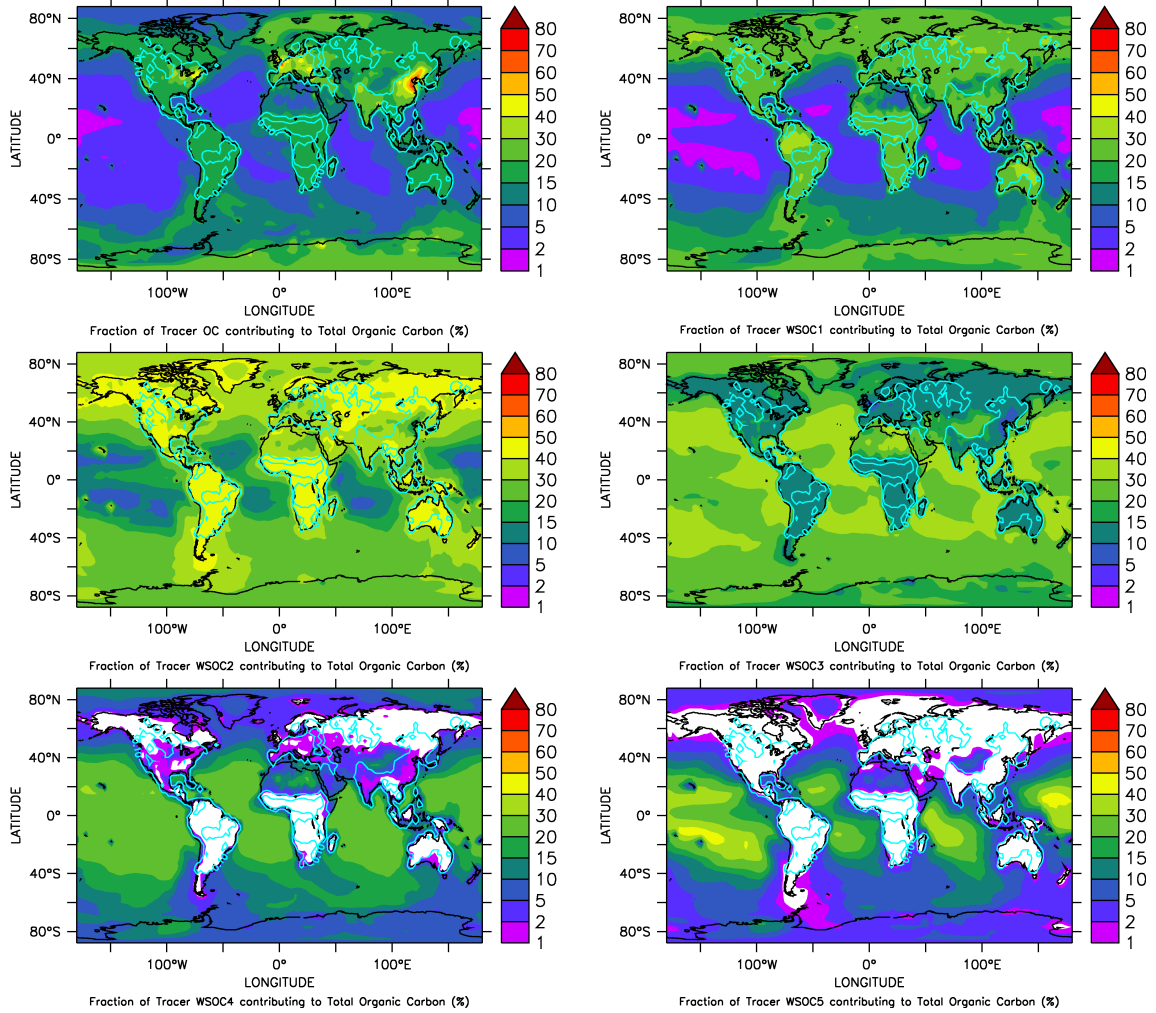


Figure 7: Annual average of the relative contribution of the different organic aerosol compounds to the total organic carbon in the surface layer. The turquoise colored line represents the total organic carbon in the layer.

3.2.2 Hydrophilic Accumulation mode

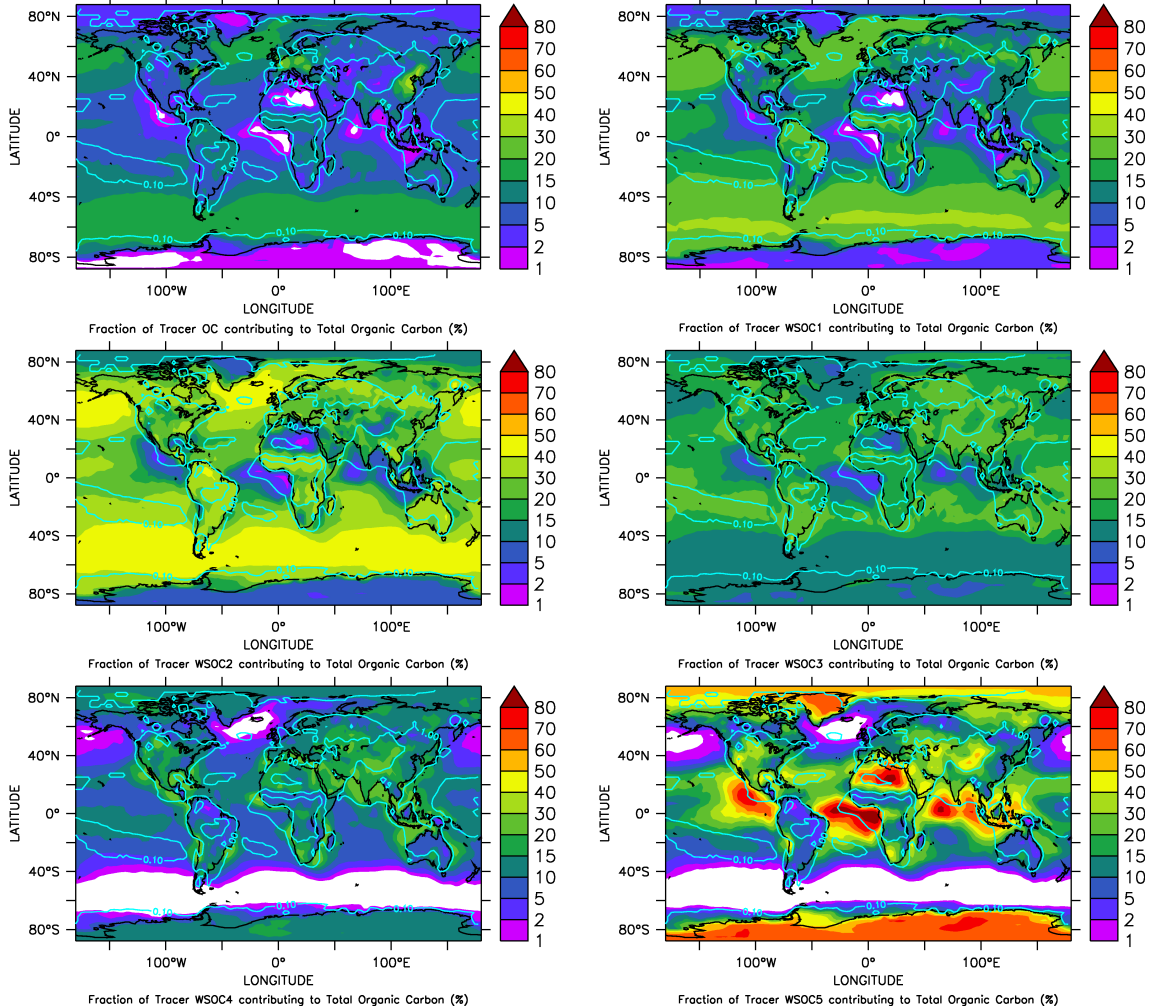


Figure 8: Annual average of the relative contribution of the different organic aerosol compounds to the total organic carbon in the surface layer. The turquoise colored line represents the total organic carbon in the layer.

3.2.3 Hydrophilic Coarse mode

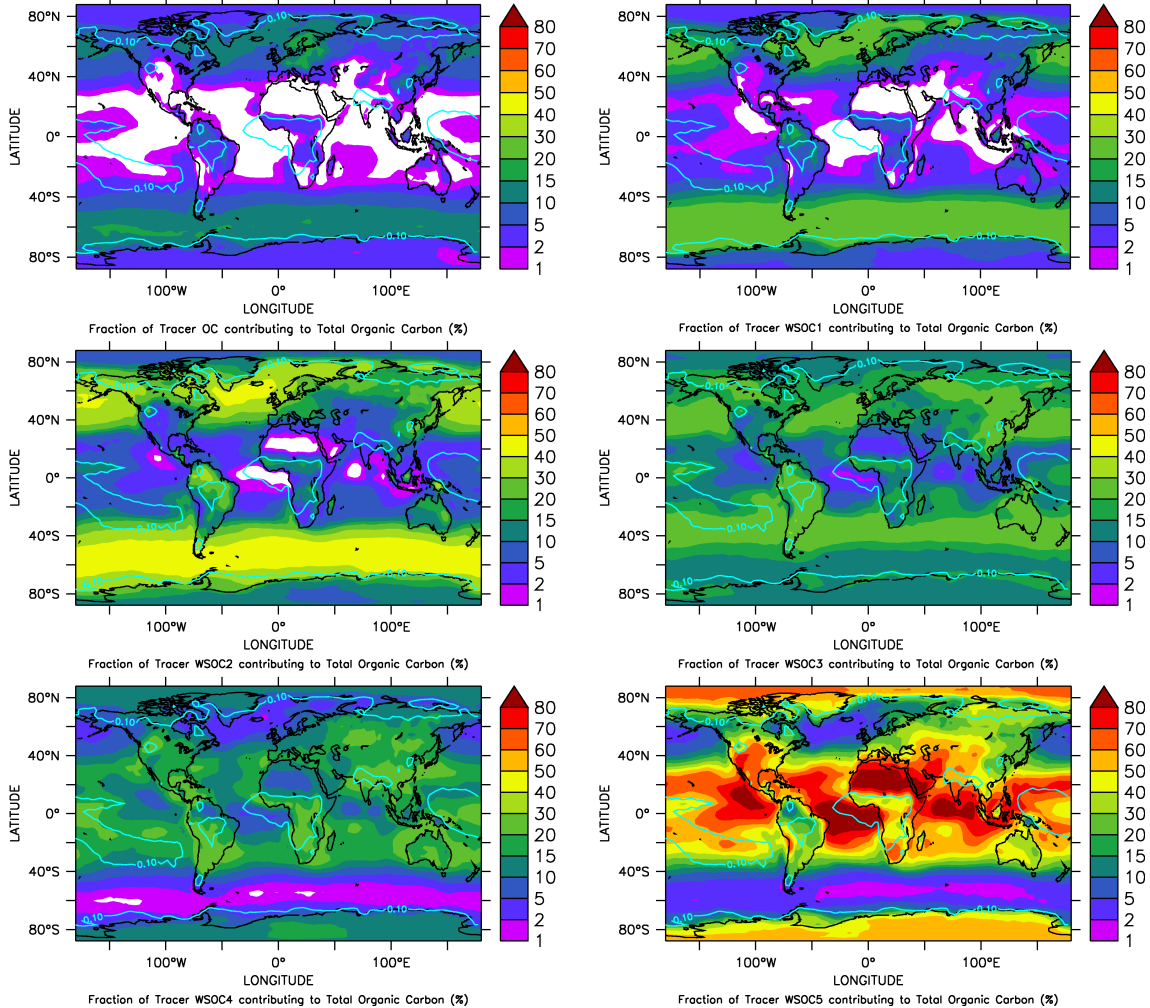


Figure 9: Annual average of the relative contribution of the different organic aerosol compounds to the total organic carbon in the surface layer. The turquoise colored line represents the total organic carbon in the layer.

3.3 Aerchem simulation

3.3.1 Hydrophilic Aitken mode

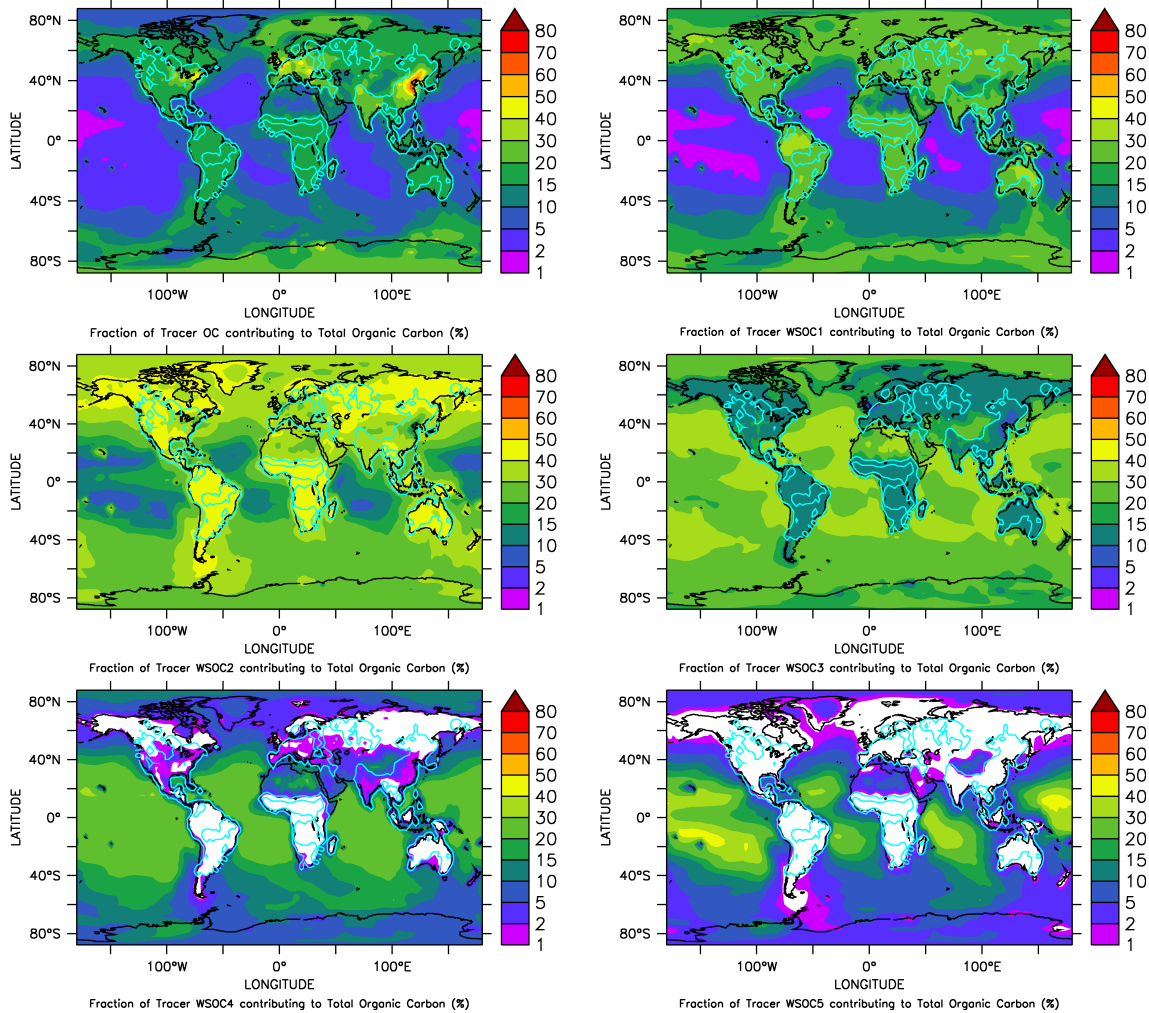


Figure 10: Annual average of the relative contribution of the different organic aerosol compounds to the total organic carbon in the surface layer. The turquoise colored line represents the total organic carbon in the layer.

3.3.2 Hydrophilic Accumulation mode

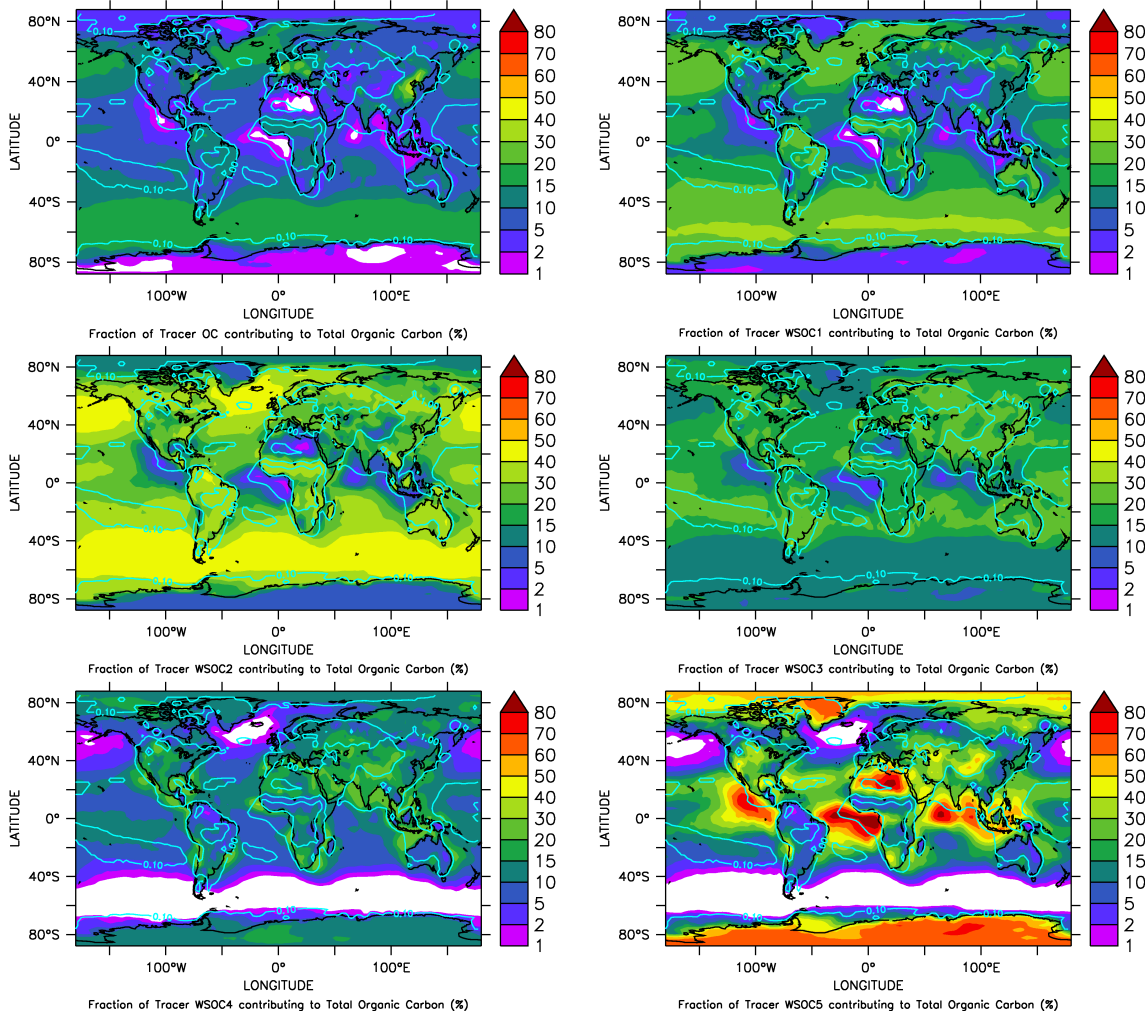


Figure 11: Annual average of the relative contribution of the different organic aerosol compounds to the total organic carbon in the surface layer. The turquoise colored line represents the total organic carbon in the layer.

3.3.3 Hydrophilic Coarse mode

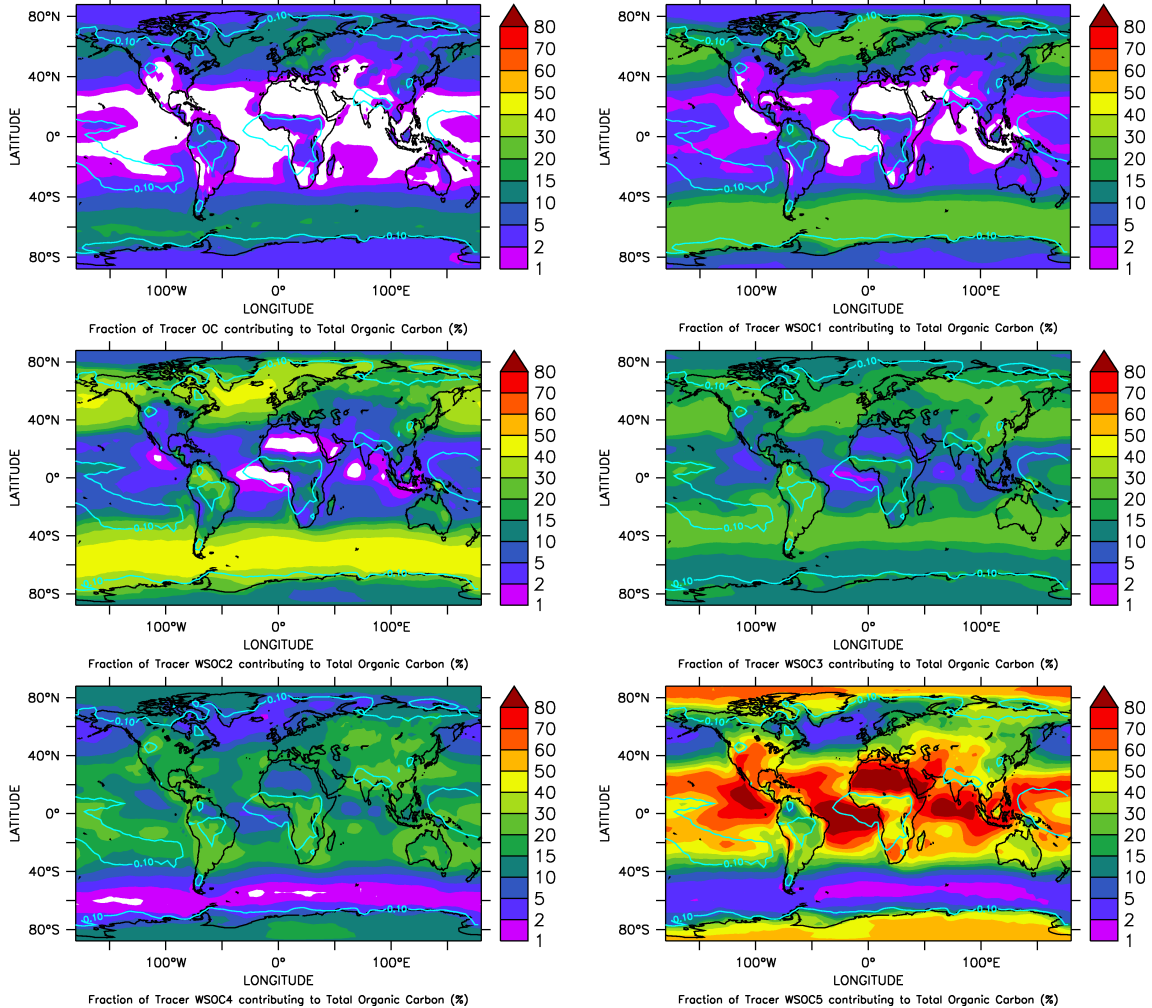


Figure 12: Annual average of the relative contribution of the different organic aerosol compounds to the total organic carbon in the surface layer. The turquoise colored line represents the total organic carbon in the layer.

3.4 *Insol* simulation

3.4.1 Hydrophilic Aitken mode

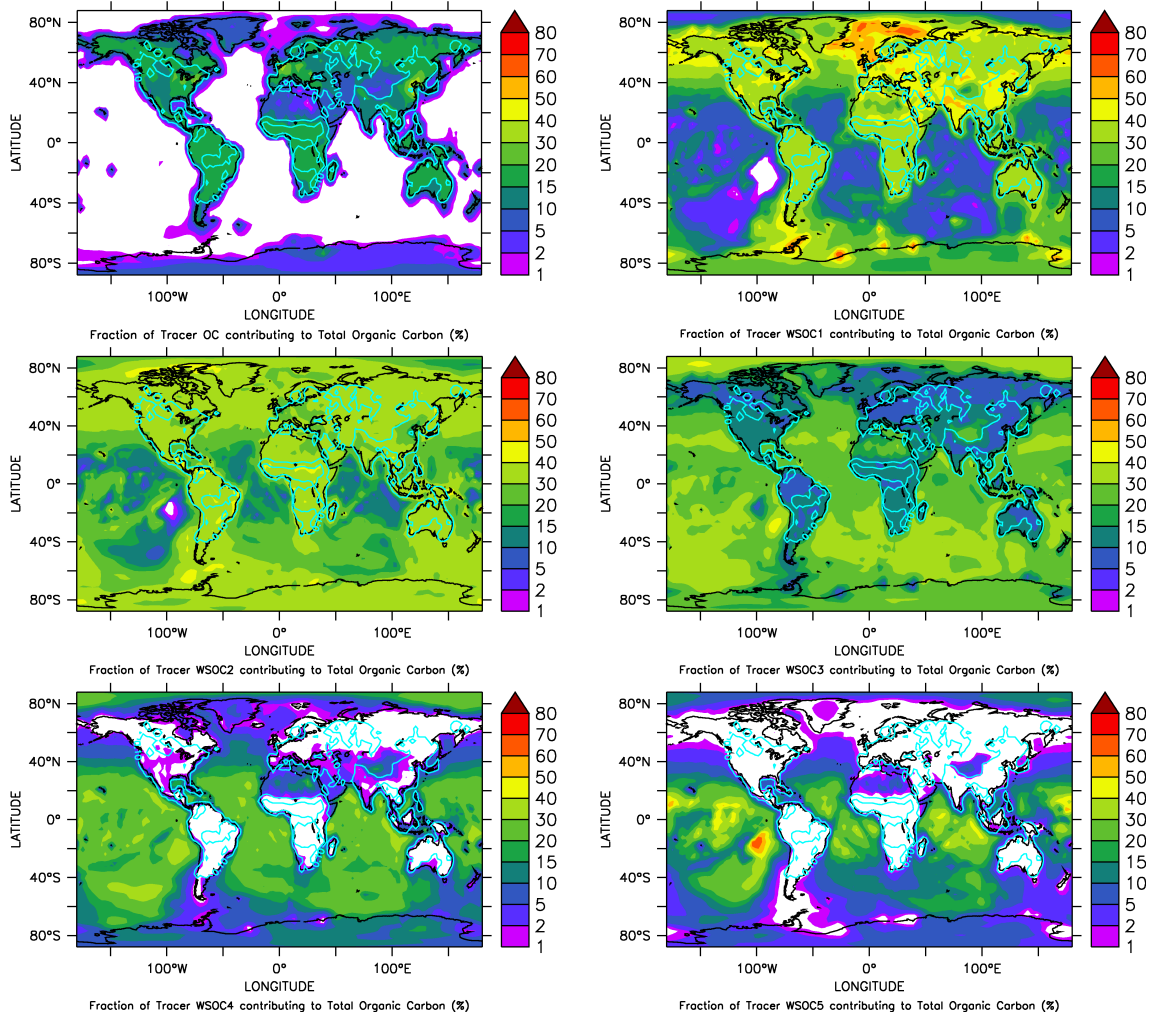


Figure 13: Annual average of the relative contribution of the different organic aerosol compounds to the total organic carbon in the surface layer. The turquoise colored line represents the total organic carbon in the layer.

3.4.2 Hydrophilic Accumulation mode

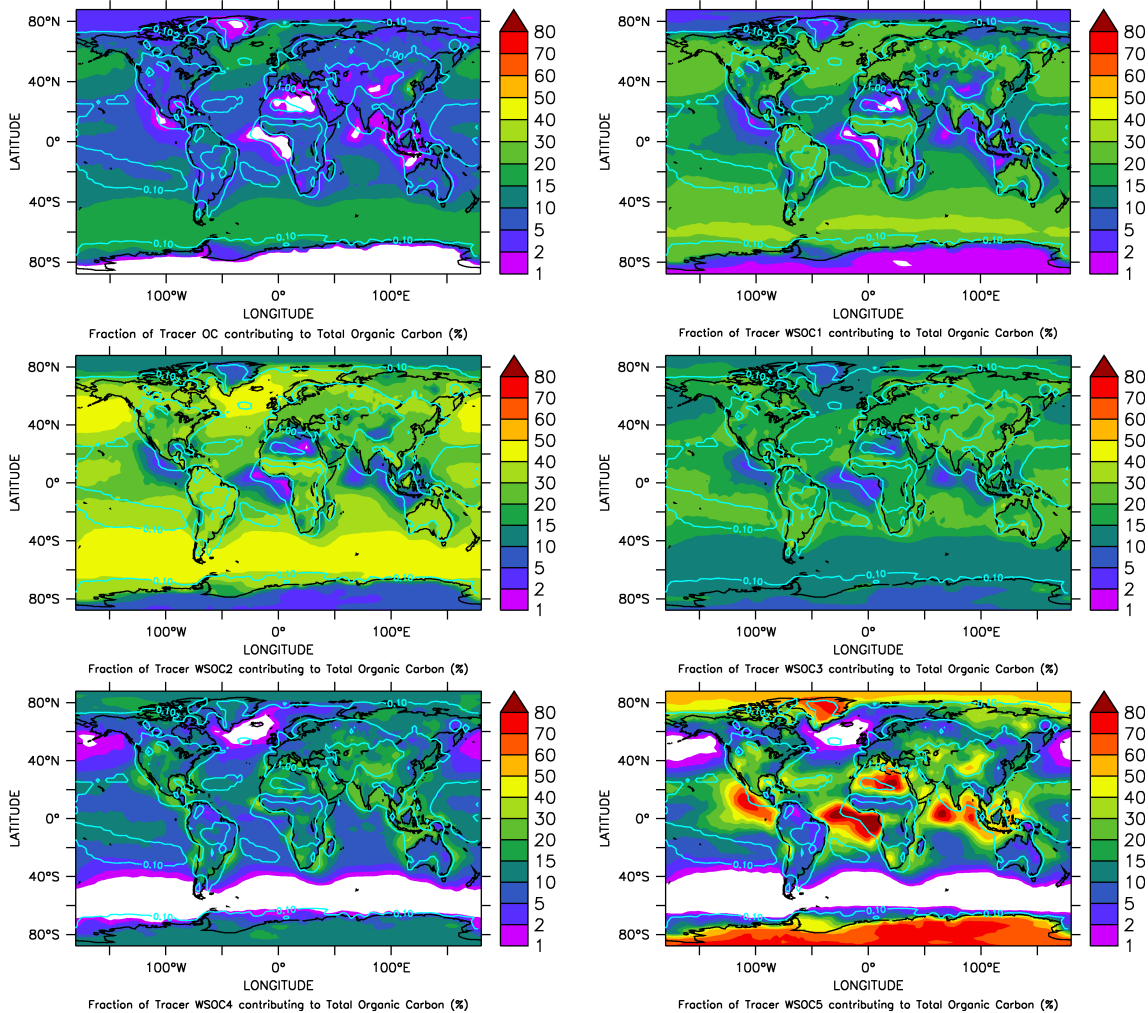


Figure 14: Annual average of the relative contribution of the different organic aerosol compounds to the total organic carbon in the surface layer. The turquoise colored line represents the total organic carbon in the layer.

3.4.3 Hydrophilic Coarse mode

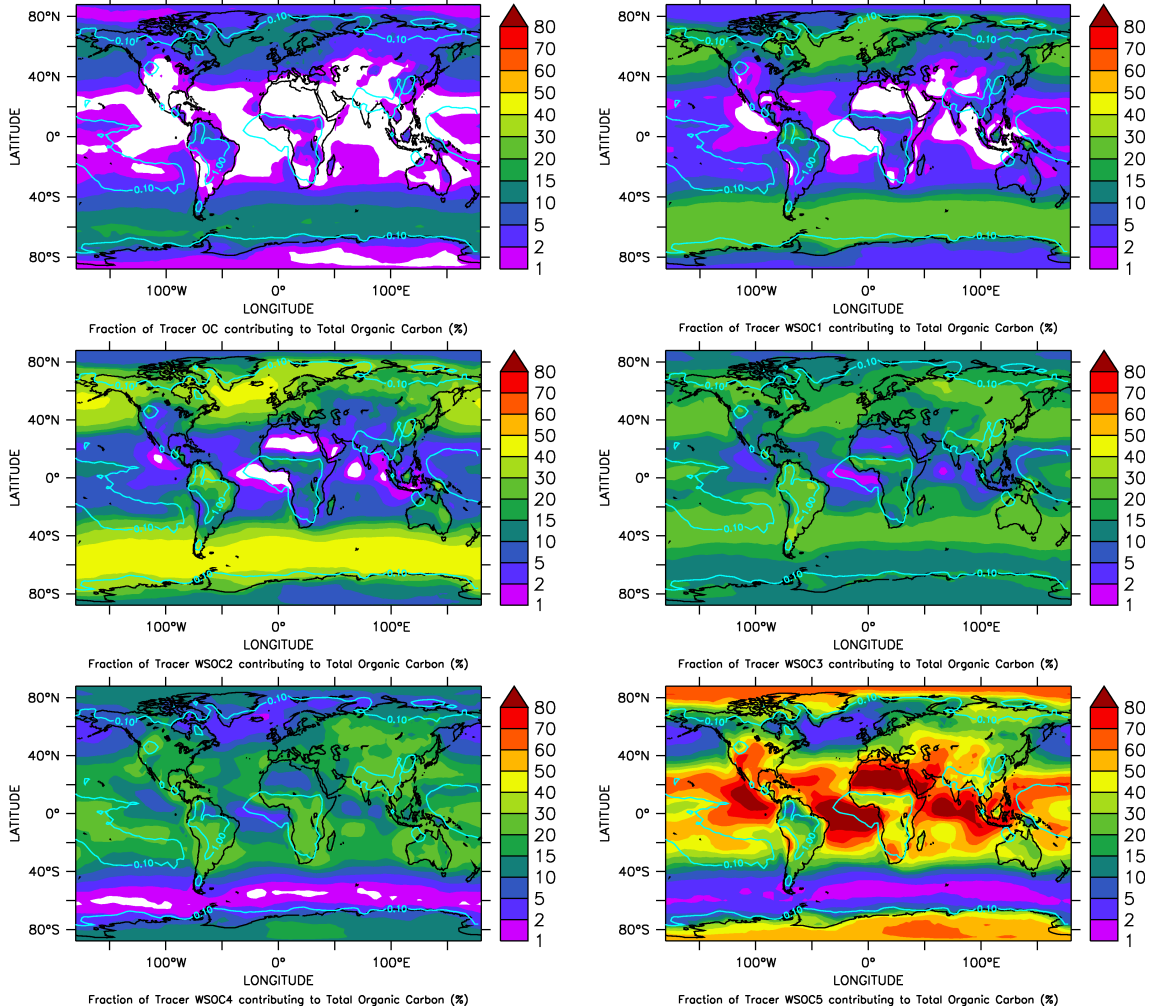


Figure 15: Annual average of the relative contribution of the different organic aerosol compounds to the total organic carbon in the surface layer. The turquoise colored line represents the total organic carbon in the layer.

4 O:C ratio differences for the *Aerchem* and *Insol* simulation

The difference plots for the O:C ratio for the two simulations not shown in the main manuscript are provided here.

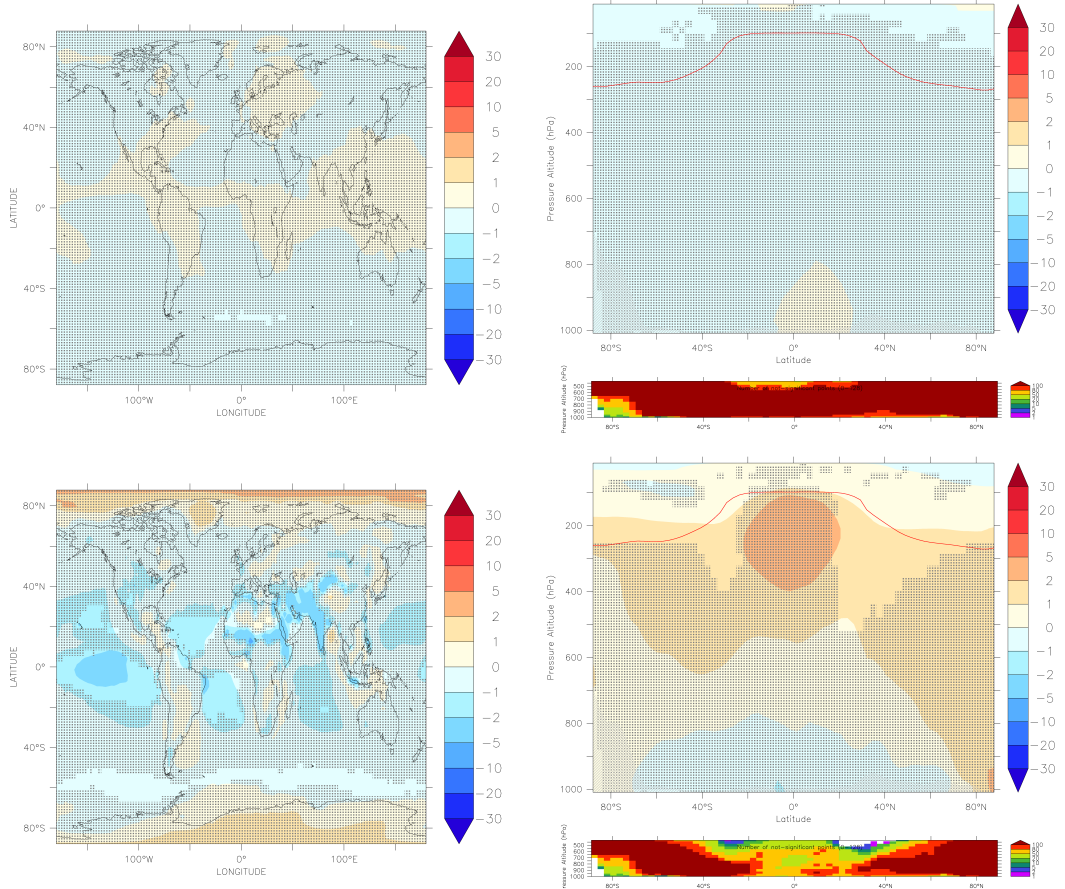


Figure 16: Annual average O:C ratio differences to the *Ageing-BG* scenario for the *Aerchem* (upper row) and the *Insol* (lower row) simulation. The left column shows the values in the surface layer, whereas the right column displays the zonal averages. Black dotted regions mark regions of low statistical significance.

5 Organic κ at PBL height for the *Aerchem* and *Insol* simulation

The difference plots for the organic κ values for the two simulations not shown in the main manuscript are provided here.

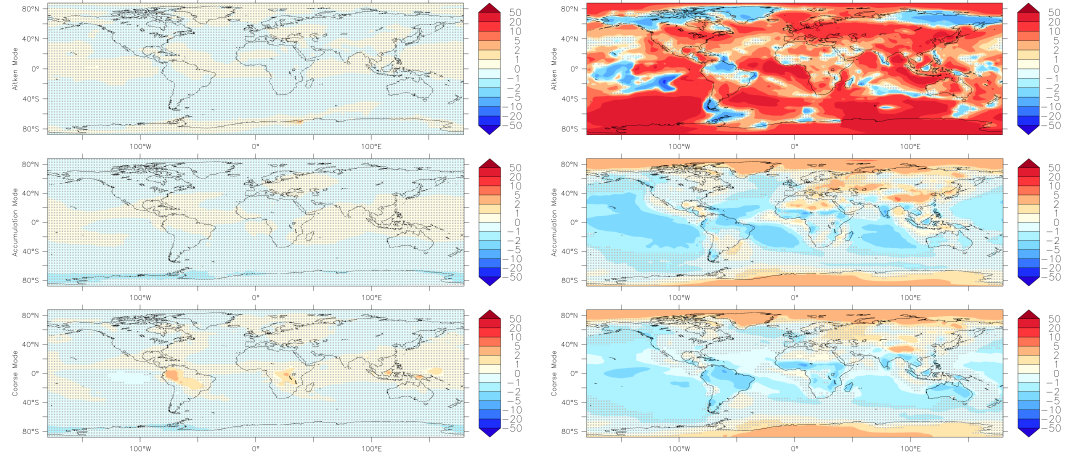


Figure 17: Annual average of the relative differences of the organic κ value to the *Ageing-BG* scenario for the *Aerchem* (left) and the *Insol* (right) simulation. The regions of low statistical significance are marked with the grey dots.

6 Organic aerosol water

The results from the simulations not shown in the main manuscript are presented here, namely the differences of the *Ageing-LO* and *Aerchem* organic aerosol water column burdens compared to *Ageing-BG*.

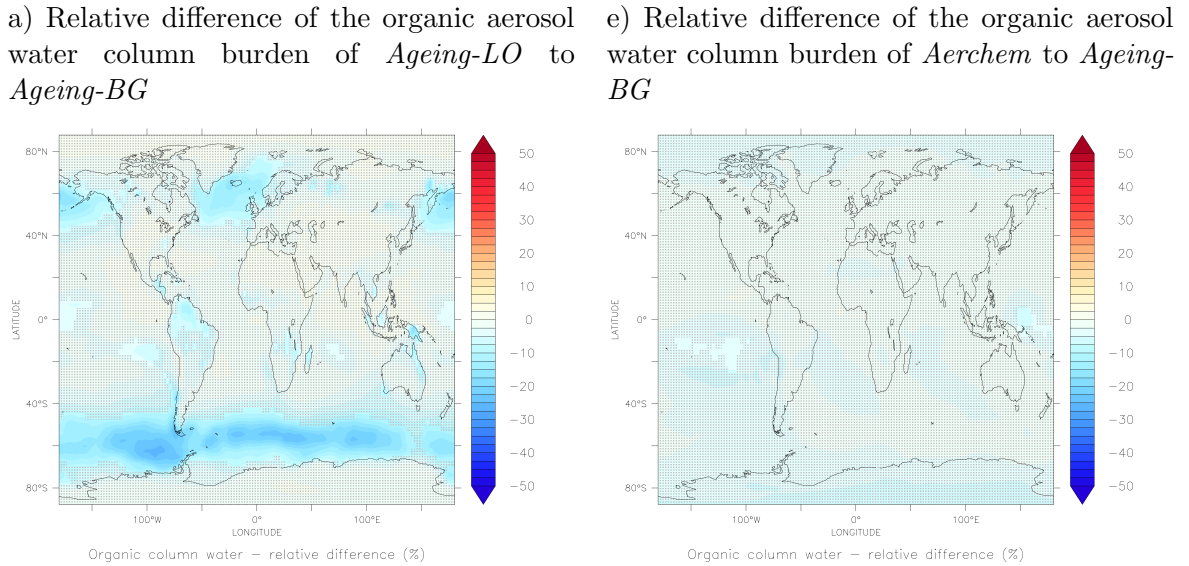
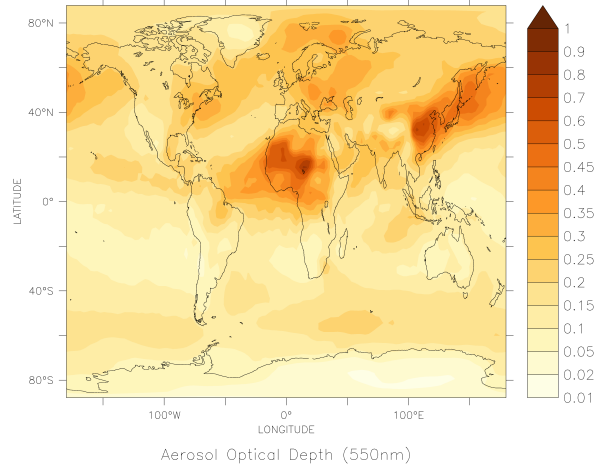


Figure 18: Annual averages of the relative differences of the organic aerosol water column burden (in mg/m²) for the *Ageing-LO* and *Aerchem* simulation to the *Ageing-BG* scenario in %; dotted areas mark regions of low statistical significance.

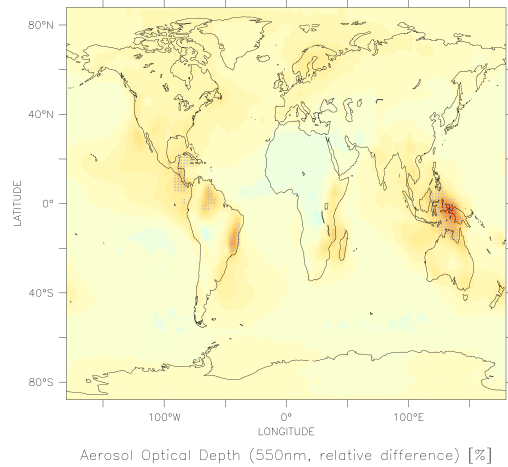
7 Aerosol optical thickness

Here, the difference plots of the aerosol optical depth are presented for the *Ageing-LO* and *Insol* simulation. For reference purposes the AOD of the *Ageing-BG* simulation is added, as shown in the main manuscript.

a) AOD in the *Ageing-BG* experiment



b) Relative difference in the AOD of *Ageing-LO* compared to *Ageing-BG*



c) Relative difference in the AOD of *Aerchem* compared to *Ageing-BG*

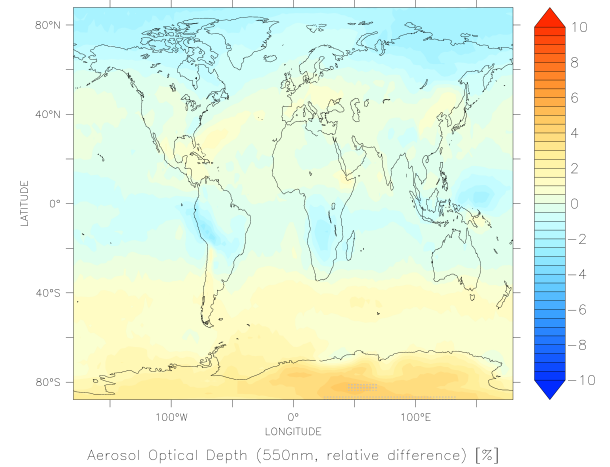
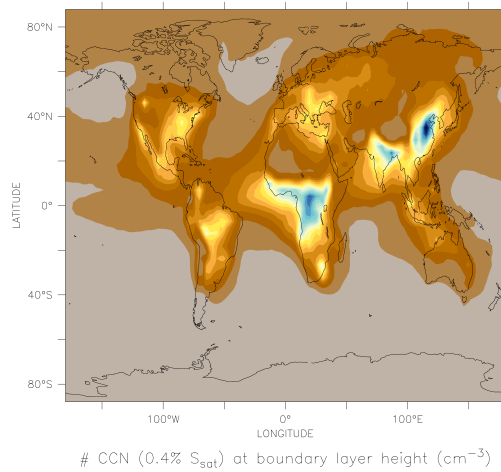


Figure 19: Annual averages of the total aerosol optical thickness. The uppermost pattern presents the absolute value for the *Ageing-BG* simulation. The panels b) and c) illustrate the relative differences of the *Ageing-LO* and *Aerchem* simulations to the reference displayed above. In contrast to previous figures dotted areas mark regions of high statistical significance.

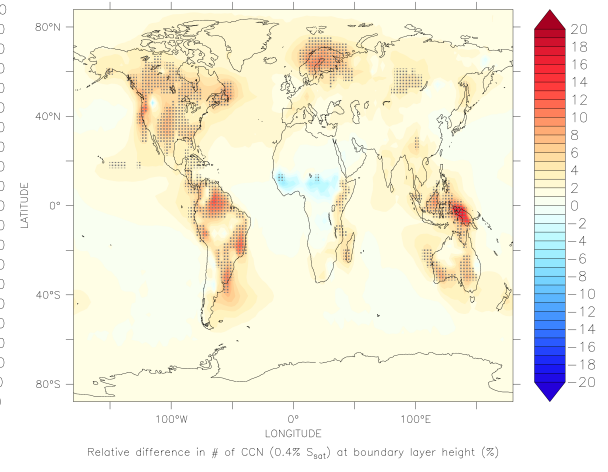
8 Cloud condensation nuclei

Here, the difference plots of the CCN at boundary layer height are presented for the *Ageing-LO*, *Aerchem* and *Insol* simulation. For reference purposes the CCN of the *Ageing-BG* simulation is added, as shown in the main manuscript.

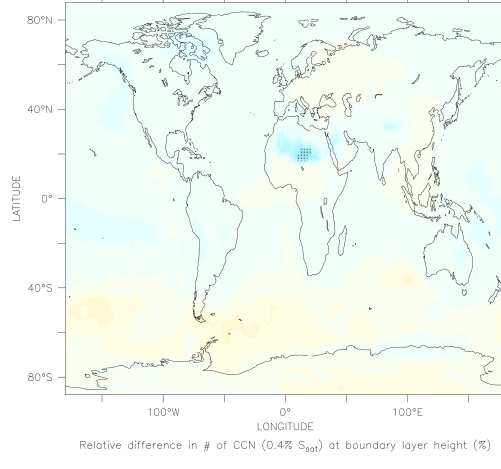
a) CCN in the *Ageing-BG* experiment



b) Relative difference in the CCN at boundary layer height of *Ageing-LO* compared to *Ageing-BG*



c) Relative difference in the CCN at boundary layer height of *Aerchem* compared to *Ageing-BG*



d) Relative difference in the CCN at boundary layer height of *Insol* compared to *Ageing-BG*

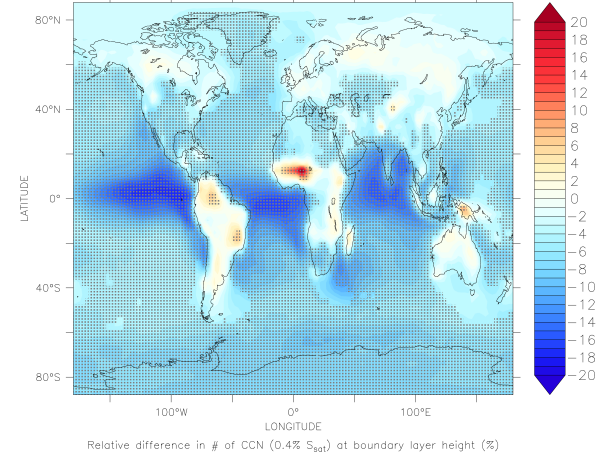


Figure 20: Annual averages of the CCN at boundary layer height calculated with an assumed supersaturation of 0.4%. The upper left panel show the absolute value for the *Ageing-BG* simulations. The upper right pattern represents the relative difference for the *Ageing-LO* simulation, and the panels in the lower row for the *Aerchem* and *Insol* experiment. Regions with high statistical significance are marked with an overlayed pattern.

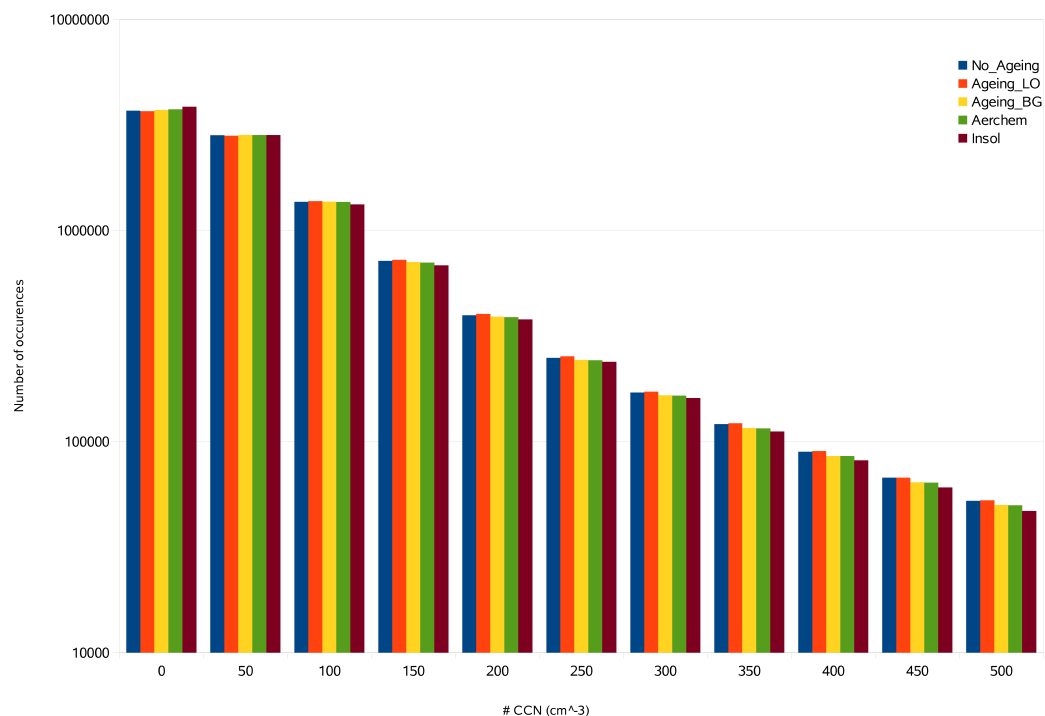


Figure 21: Histogram for the CCN distribution for low CCN values in the five simulations denoted by the different colours.

Additionally the histogram for the occurrences of low CCN numbers is provided.

References

- Pringle, K. J., Tost, H., Metzger, S., Steil, B., Giannadaki, D., Nenes, A., Fountoukis, C., Stier, P., Vignati, E., and Lelieveld, J.: Description and evaluation of GMXe: a new aerosol submodel for global simulations (v1), Geoscientific Model Development, 3, 391–412, 2010.